

FLOW AND ACOUSTIC NOISE OF SINGLE STREAM SUBSONIC JETS FROM NOZLES WITH AND WITHOUT CHEVRONS

Rafael Costa Engel, engel@polo.ufsc.br

Cesar J. Deschamps, deschamps@polo.ufsc.br

POLO Research Laboratories for Emerging Technologies in Cooling and Thermophysics
Federal University of Santa Catarina
88040-900, Florianópolis, Brazil

Carlos Roberto Ilário da Silva, carlos.ilario@embraer.com.br

EMBRAER SA
São José dos Campos, Brazil

Abstract. Numerical predictions of the flow field and acoustic noise of jets from nozzles with and without chevrons have been obtained for Mach number $M=0.9$ and Reynolds number $Re=1.38 \times 10^6$. The fluid flow simulations were based on two turbulence models, a Reynolds stress transport model (RSTM) and a cubic $k-\varepsilon$ model. A hybrid approach was adopted for noise prediction, with turbulence statistics, such as length and time scales, being obtained from the fluid flow solution and used as input for two methods of noise prediction: the waveprop1 method available in the code CAA++ and the Lighthill Ray-Tracing (LRT) method developed by Silva *et al.* (2011). Both methods are based on the Lighthill's acoustic analogy, but differ from each other in the way noise source terms are evaluated and sound pressure waves are propagated to the far-field. It has been verified that only the LRT method is capable of providing predictions for the noise spectra at the far field in close agreement with experimental data.

Keywords: Chevron nozzle, aeroacoustics, jet noise.

1. INTRODUCTION

Chevron nozzles are passive methods adopted in aircraft engines to modify the noise spectrum by changing the characteristics of the turbulent flow. Many chevron nozzle geometries have been studied in the literature in order to identify their influence on the flow and acoustic fields. For instance, Bridges and Brown (2004) carried out an experimental study of ten nozzle geometries and their measurements have been widely used for assessing different numerical models developed to predict the flow and acoustic fields.

The most straightforward technique to simulate turbulent flows is via the direct solution of the Navier-Stokes equations with a suitable numerical algorithm, referred to as Direct Numerical Simulation (DNS). However, the computational resources, in terms of memory and speed, needed to resolve the smallest time and space scales of the turbulent motion of engineering flows cannot be supplied by present computers. Large-Eddy Simulation (LES) solves only large scales, while effects of the small eddies are modeled. LES is much less expensive than DNS but still too expensive for industry applications. For this reason, most simulations of turbulent flows adopt a statistical description of the flow in which any instantaneous property is expressed in terms of an average quantity plus fluctuations about the average. This class of modeling gives rise to the so called Reynolds Averaged Navier-Stokes equations (RANS).

The acoustic field can also be directly solved by using a computational grid large enough to encompass the observer so that the pressure fluctuations can be evaluated at the desired point. The method is called direct because the sound pressure fluctuations are obtained directly from a transient solution of the flow field via DNS or LES. Another option is to adopt a hybrid simulation approach to reduce computational domain, in which an acoustic method is required to propagate the acoustic pressure from the near field to the observer in the far field.

Engblom *et al.* (2004) adopted a hybrid approach with the SST turbulence model to predict the flow field and the Lilley equations to propagate the resulting noise. Overall, the authors obtained predictions in good agreement with the experimental data. Birch *et al.* (2006) used the $k-\varepsilon$ model with modified constants as an attempt to improve agreement with measurements of Bridges and Brown (2004). The present study considers the numerical simulations of the flow and acoustic noise of a single stream jet flow from nozzles with and without chevrons, with Mach number $M=0.9$ and Reynolds number $Re=1.38 \times 10^6$. The Reynolds Stress Transport model (RSTM) and the cubic $k-\varepsilon$ model were adopted in the simulations in combination with two aeroacoustic methods. The first one is the waveprop1 method implemented in the code CAA++ (Metacomp Inc., 2009). The other approach is the Lighthill Ray Tracing (LRT) method proposed by Silva *et al.* (2011).

2. PROBLEM DESCRIPTION AND COMPUTATIONAL DETAILS

The nozzles SMC000 (without chevron) and SMC0006 (with chevron) investigated in the present work are those adopted in the measurements of Bridges and Brown (2004). Both nozzles are depicted in Fig. 1 and their geometric characteristics are given in Table 1. The chevron nozzle SMC0006 was chosen because of its high penetration into the

flow, which modifies dramatically the jet development. In Table 1, N stands for the number of chevrons, C is the length of the chevron, θ is the penetration angle, D_e is the effective diameter of the nozzle and P is the penetration, given by the difference between the diameters of the nozzle base and nozzle tip. Figure 2 shows the nozzle inlet and outlet diameters. All the dimensions are in millimeters.

The inlet boundary conditions for the simulations were based on the measurements of Bridges and Brown (2004). At the inlet, the stagnation temperature and the stagnation pressure were imposed ($T_e = 288\text{K}$ and $p_e = 178.2\text{kPa}$). However, no information was available for the turbulence quantities. The square root of the inlet area was used as an estimate of the turbulence length scale (L) and a turbulence intensity of 2% was assumed in all simulations. As far as the initial flow field is concerned, a value of 1 m/s was adopted for the axial component of velocity, U_{0x} , while the other two components (U_{0y} e U_{0z}) were set to zero. The initial conditions for pressure and temperature were $p_a = 97.7\text{kPa}$ and $T_a = 280.2\text{K}$.



Figure 1. Nozzle geometries studied by Bridges and Brown (2004).

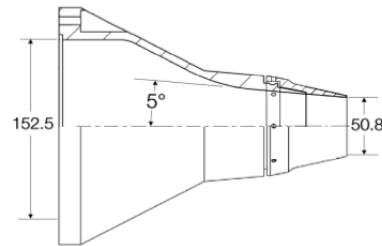


Figure 2. Nozzle overall geometry.

Table 1. Geometric parameters of the nozzles.

Nozzle	N	C (mm)	θ (°)	P (mm)	D_e (mm)
SMC000	0	-	-	-	50.4
SMC006	6	22.6	18.2	3.52	47.7

Tests of grid refinement were carried out for each nozzle in order to assess truncation error. Three grids with 4×10^6 , 8×10^6 and 16×10^6 elements were tested for the nozzle SMC000. Since no significant difference was noticed between the results of turbulence quantities and mean velocity obtained with such grids, the less refined and computationally less expensive grid was chosen for the simulations. A similar procedure was adopted for the nozzle SMC006 and a grid with 4×10^6 elements was also chosen for the final simulations.

The fluid flow simulations in the present study are based on two turbulence models, a Reynolds stress transport model (RSTM) and a cubic $k-\varepsilon$ model that are implemented in the commercial code CFD++ (Metacomp Inc., 2009). On the other hand, two aeroacoustic methods were applied to predict the sound pressure level (SPL) spectrum at an observer located in the far-field at 100 diameters distant from the nozzle lip: i) the waveprop1 method implemented in the code CAA++ (Metacomp Inc., 2009); ii) the Lighthill Ray Tracing (LRT) method proposed by Silva *et al.* (2011). Both methods are based on the Lighthill's acoustic analogy (Lighthill, 1951), but differ from each other in the way noise source terms are evaluated and sound pressure waves are propagated to the far-field.

3. RESULTS

Results are provided for flow and acoustic fields. Turbulence quantities are the most relevant results for the acoustic simulation and, therefore, such quantities are carefully analyzed. Results for spectra of sound pressure level (SPL) in the far-field of the jet are presented and compared with experimental data.

3.1 Fluid Flow

Figure 3 shows numerical results for velocity along the centerline of the jets from the nozzles SMC000 and SMC006 and the corresponding experimental data of Bridges and Brown (2004). As can be seen, the reduction of the length of the potential core brought about by chevron nozzle is correctly predicted, although such a length is over estimated in both nozzles.

The axisymmetric flow condition verified for the nozzle SMC000 does not hold for the nozzle SMC006. Therefore, results are presented along the lines Y-Y' and Z-Z' for the jet from the chevron nozzle (Fig. 4), corresponding to lines from tip to tip and from valley to valley of the chevron petal.

Turbulence quantities are particularly important in the prediction of acoustic noise. Figures 5, 6 and 7 depict results of normal Reynolds stresses \overline{uu} , \overline{vv} , and \overline{ww} for the cross-sections located at $x/D_j = 2, 5$ and 10 along the jet potential core. It should be mentioned that the position at $x/D_j = 10$ is in the region responsible for most of the sound generation.

By examining the results for \overline{uu} , \overline{vv} , and \overline{ww} , one can see that the simulations predicted an asymmetry condition ($\overline{vv} \neq \overline{ww}$) at $x/D_j = 2$ for the jet from the chevron nozzle and a trend to an axisymmetric condition ($\overline{vv} \cong \overline{ww}$) beyond $x/D_j = 5$. This phenomenon, also observed experimentally, is a consequence of the fact that chevrons increase turbulent diffusion in the jet.

Another important effect of chevrons that was predicted in agreement with measurements is the higher turbulence intensity near the nozzle exit and the lower turbulence intensity at the end of the potential core. In fact, the enhancement of jet mixing at the exit of the chevron nozzle gives rise to higher dissipation rate and, hence, to lower levels of turbulence kinetic energy near the end of the jet potential core, where the most significant sound sources are usually generated.

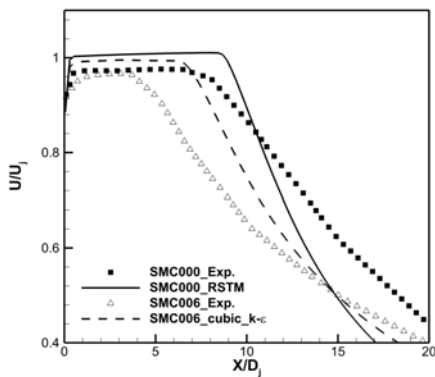


Figure 3. Mean velocity along the jet centerline.

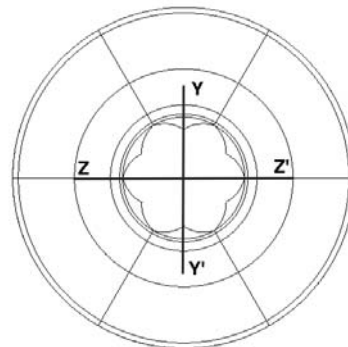


Figure 4 – Cross-section lines of chevron nozzles.

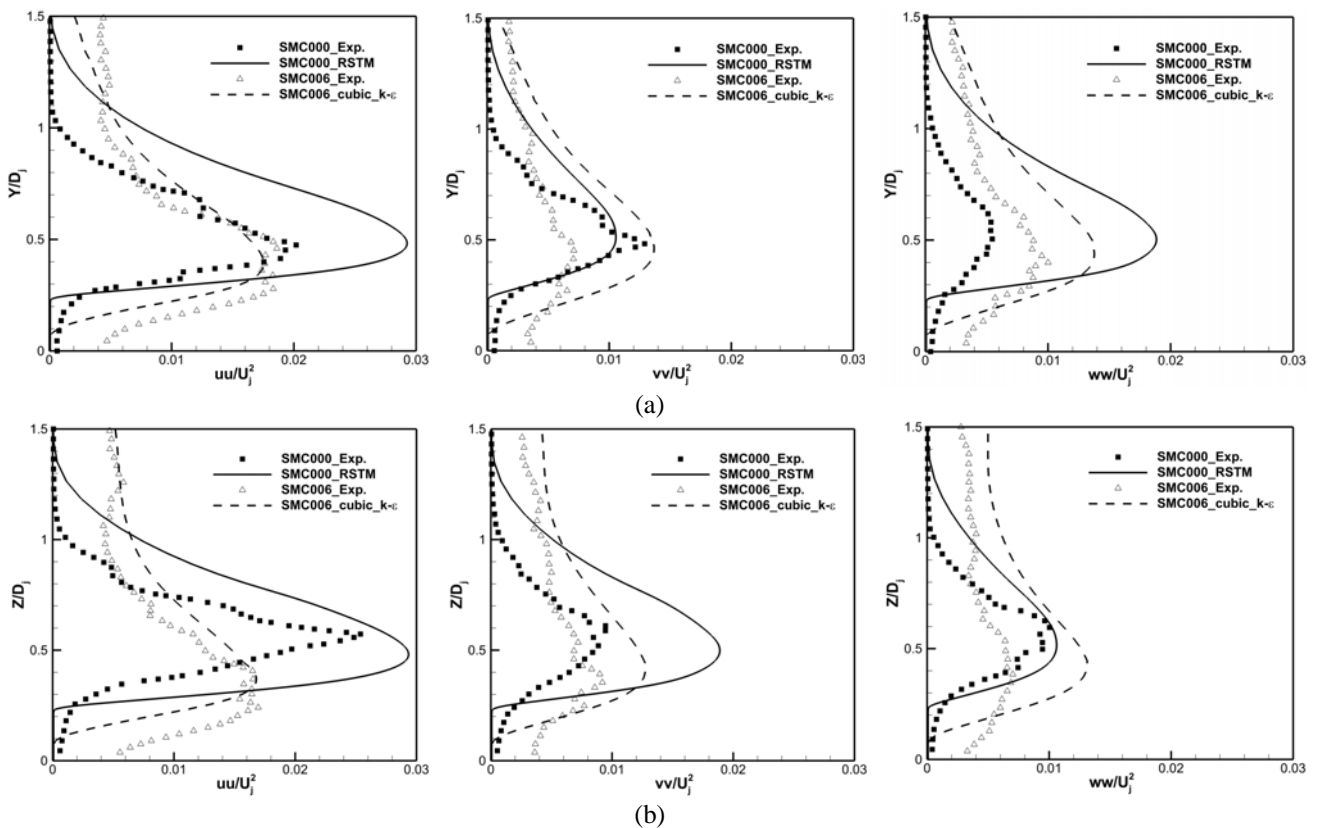


Figure 5. Normal Reynolds stresses at $x/D_j = 5$; (a) Y-Y' cross-section; (b) Z-Z' cross-section.

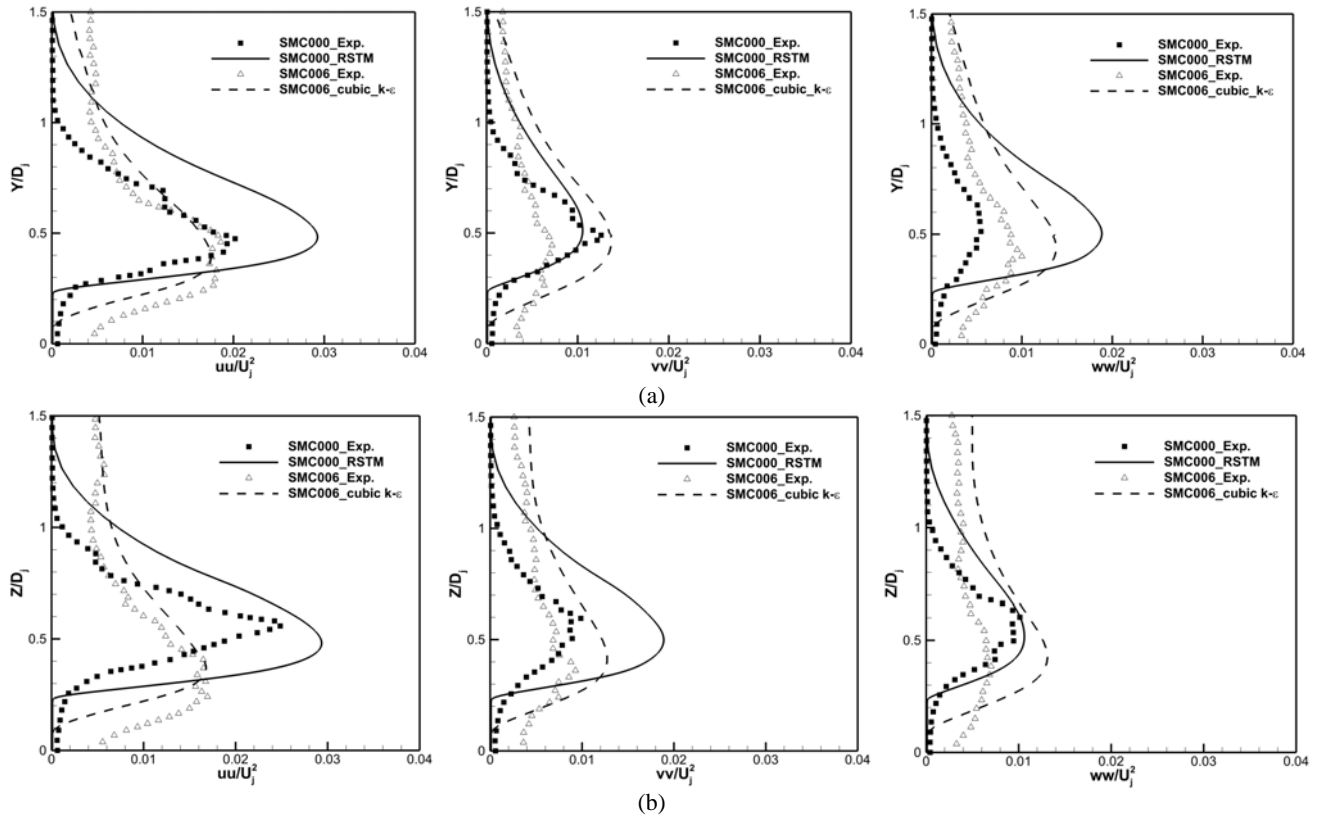


Figure 6. Reynolds stress components at $5 D_j$. (a) Y-Y' cross-section; (b) Z-Z' cross-section.

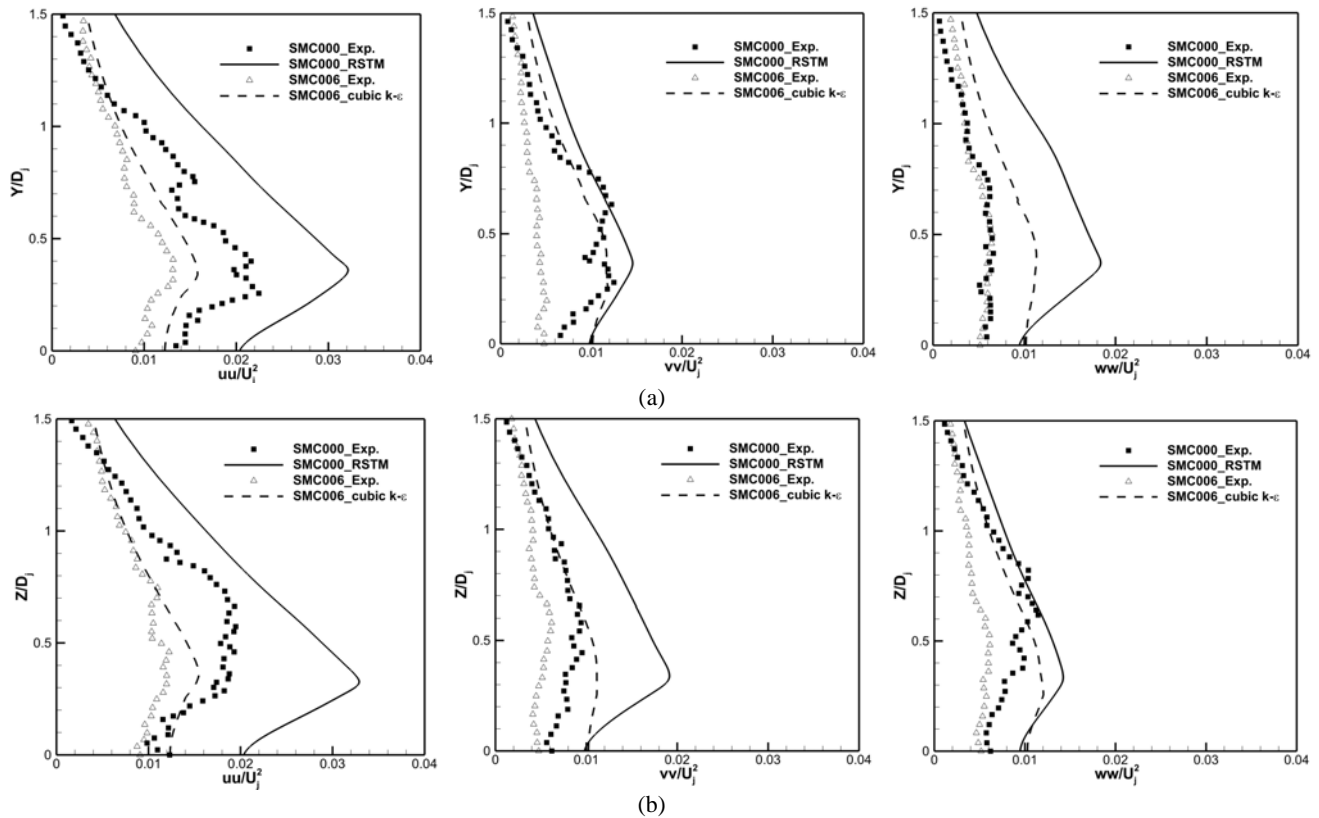


Figure 7. Reynolds stress components at $10 D_j$. (a) Y-Y' cross-section; (b) Z-Z' cross-section.

3.2 Acoustic Noise

Following the hybrid approach for noise prediction, a post-processing step based on aeroacoustic theory must be carried out. In the present study, the fluid flow solution was used as an input for two methods of noise prediction: i) the wavepro1 method available in the code CAA++ and ii) the LRT method developed by Silva *et al.* (2011).

Figures 8 and 9 show numerical and experimental results of sound pressure level (SPL) spectrum for an observer located at $100 D_j$ distant from the nozzles SMC000 and SMC006, respectively, with an angle of 90° relative to the jet centerline. The results obtained with the LRT model are in much better agreement with the experimental data than those predicted with the wavepro1 method, despite some discrepancy at low and high frequency for the nozzle SMC000. The poor predictions of the wavepro1 seem to be associated with deficiencies in the turbulence reconstruction technique used to obtain the velocity fluctuations that characterize the sound sources.

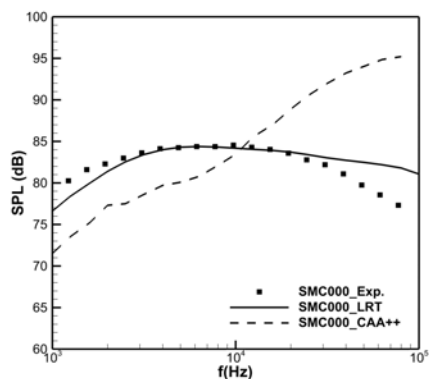


Figure 8. Acoustic spectra observed at 90° and $100 D_j$ distant from de nozzle lip for SMC000.

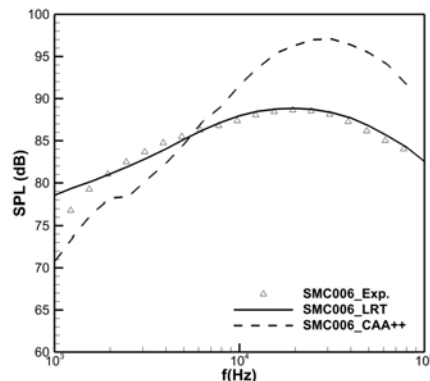


Figure 9. Acoustic spectra observed at 90° and $100 D_j$ distant from de nozzle lip for SMC006.

4. CONCLUSIONS

Simulations of single-stream subsonic jets from nozzles with and without chevrons were carried out with two RANS turbulence models: a cubic $k-\varepsilon$ model and a Reynolds stress transport model (RSTM). The results showed that both models are able to predict high speed jets from different nozzle geometries. For instance, the reduction of the jet potential core length brought about by chevron nozzles was predicted in line with experimental observation. A hybrid aeroacoustic approach in which the fluid flow field and the acoustic field are solved in a segregated manner was adopted to predict the sound pressure level (SPL) at the far field. The wavepro1 method available in the code CAA++ was not able to predict SPL in agreement with experimental data, arguably because of deficiencies in the method used to reconstruct the instantaneous turbulent field from RANS simulations. On the other hand, the LRT model predicted results in reasonable agreement with measurements, encouraging its application in the analysis of other nozzle geometries and sound directivity.

5. REFERENCES

- Birch, S.F., Lyubimov, D.A., Maslov, V.P. and Secundov, A.N., 2006. "Noise prediction chevron nozzle". 12th AIAA/CEAS Aeroacoustics Conference, Cambridge, Massachusetts, USA, Paper AIAA 2006-2600.
- Bridges, J. and Brown, C.A., 2004. "Parametric testing of chevrons on single flow hot jets". 10th AIAA/CEAS Aeroacoustics Conference, Manchester, UK, Paper AIAA 2004-2824.
- Engblom, W. A., Khavaran, A. and Bridges, J., "Numerical prediction of chevron nozzle noise reduction using WIND-MGBK methodology". 10th AIAA/CEAS Aeroacoustics Conference, Manchester, UK, Paper AIAA 2004-2979.
- Lighthill, M.J. On sound generated aerodynamically: I. General theory. Proceedings of the Royal Society of London, 1951.
- Metacomp Technologies INC. "User's manual". 2009.
- Silva, C.R.I, Meneghini, J. R., Azarpeyvand, M. and Self, R.H., 2011. "Refraction effects on far-field noise predictions and sources distribution of coplanar coaxial jet flows". 17th AIAA/CEAS Aeroacoustics Conference, Portland, Oregon, USA, Paper AIAA 2011-2749.

6. RESPONSIBILITY NOTICE

The authors are the only responsible for the printed material included in this paper.